

# Applying higher-modes consistency test on GW190814 : lessons on no-hair theorem, nature of the secondary compact object and waveform modeling

Tousif Islam<sup>1,2,3,4,\*</sup>

<sup>1</sup>Center for Scientific Computing and Visualization Research, University of Massachusetts, Dartmouth, MA 02747, USA

<sup>2</sup>Department of Physics, University of Massachusetts, Dartmouth, MA 02747, USA

<sup>3</sup>Department of Mathematics, University of Massachusetts, Dartmouth, MA 02747, USA

<sup>4</sup>Kavli Institute for Theoretical Physics, University of California, Santa Barbara, CA 93106, USA

(Dated: November 2, 2021)

As one of the consequences of the black-hole “no-hair” theorem in general relativity (GR), the multipolar structure of the radiation (i.e. different spherical harmonic modes) from a merging quasi-circular binary black hole (BBH) is fully determined by the intrinsic parameters (i.e. the masses and spins of the companion black holes). In Refs. [1, 2], we have formulated an efficient test named ‘higher-modes consistency test’ to check for the consistency of the observed gravitational-wave (GW) signal with the expected multipolar structure of radiation from BBHs in GR. Detection of the high-mass-ratio merger of GW190814 enables the observation of spherical harmonic modes beyond the dominant  $(\ell, m) = (2, \pm 2)$  mode; thereby providing a unique opportunity to perform the ‘higher-modes consistency test’. Using different state-of-art waveform models (IMRPhenomXPHM, IMRPhenomXHM, IMRPhenomHM and SEONNRv4HM\_ROM), we show that GW190814 strongly favors the “no-hair” hypothesis in GR over a hypothesis that assumes generic deviation from the multipolar structure of the radiation by a Bayes factor of  $\log_e \mathcal{B} \sim 8$ . We further investigate any potential systematic errors arising as a result of different waveform modeling choices as well as due to neglecting many higher order modes. We find that, if the waveform model includes only  $(\ell, m) = (3, \pm 3)$  mode in its higher harmonics, the same event may reject the ‘no-hair’ hypothesis in GR when the detector sensitivity improves by a factor of 12.5. Our analysis, therefore, provides motivation to include as many higher order modes as possible in future waveform models.

## I. INTRODUCTION

GW190814 [3, 4] is the highest mass ratio binary merger event detected by the LIGO [5]-Virgo [6] collaboration so far. The original LVC analysis constrains the mass ratio to be  $q := m_1/m_2 \sim 8.9$  [3] (where  $m_1$  and  $m_2$  are the component masses for the binary with  $m_1 > m_2$ ). Observation of GW190814 is also unique in the sense that the secondary object has a mass of  $2.6M_\odot$  - which lies in the hypothesized ‘lower mass gap’ [7–10] defined by the theoretically possible highest mass for a neutron star and the lowest possible mass for a black hole. Till date, the exact nature of the secondary is still unclear [11–26]. This prompted fresh looks in understanding possible formation channels for this binary [27–30] and its implications in alternate theories of gravity [31–33]. Such asymmetric mass-ratio systems excite several higher order harmonics of the gravitational radiation. The official LVC analysis [3] have been able to find strong support for the  $(\ell, m) = (3, \pm 3)$  spherical harmonics modes in the signal apart from the dominant quadrupolar  $(\ell, m) = (2, \pm 2)$  modes. GW190814 therefore provides an excellent opportunity to probe beyond the dominant multipole of the GW signal. This event is particularly suited for performing a specific kind of null tests of binary black holes in general relativity (GR) - which we call the ‘higher modes consistency’ tests [1, 2].

‘Higher modes consistency’ test is one of the null tests of GR or of binary black hole nature [34–54]. The test exploits a generalized version of ‘no-hair theorem’ for binary black holes in GR. “No-hair” theorem in GR states that a stationary

black hole can be fully described solely by its mass, spin angular momentum and electric charge [55–57]. As astrophysical black-holes are unlikely to possess electric charge, a stationary black hole can be fully described by only its mass and spin. As a consequence of this theorem, the gravitational radiation from a perturbed black hole can also be fully described by its masses and spins. This implies that the frequencies and damping times of the quasi-normal modes [58–60] of the gravitational radiation from a perturbed black hole are fully determined by these parameters. This allows us to construct a test of ‘no-hair theorem’ where we estimate the masses and spins of the perturbed black hole using different quasi-normal modes and compare those estimates against each other to check for consistency. If ‘no-hair theorem’ is correct, these estimates have to be consistent with each other; otherwise it will indicate a potential violation of the no-hair theorem [61]. This exercise is popularly known as ‘black-holes spectroscopy’ [52, 61–68].

Similarly, the gravitational radiation from a merging binary black hole can be uniquely determined in GR by a small set of parameters: masses and spins of the black holes and orbital parameters. As most binaries are expected to be circularized by the time it enters the LIGO-Virgo sensitivity band, we can safely ignore the eccentricity parameters. This implies that different spherical harmonic modes of the radiation have to be consistent with the same values for this small set of parameters. Thus, the consistency between the estimated values from different modes of the observed signal provides a test similar to the ‘black-holes spectroscopy’. Inconsistencies between different spherical harmonic modes would point to departure from the multipolar structure of radiation as expected from a binary black hole merger in GR. Such a violation would indicate that either the signal is produced by non-binary black hole compact objects or the underlying theory of gravity is not

\* tislam@umassd.edu

GR or the signal might have been modified by astrophysical phenomena such as lensing of GW signal [69] or environmental effects [70–73]. In Refs. [1, 2], we have developed two such tests (that we refer to as ‘higher modes consistency’ tests) that can efficiently check for possible inconsistencies in different spherical harmonic modes of the observed GW signal by introducing generic deviation parameters for the masses in the higher order modes. Similar test [74] have recently been applied to GW190412 [75] and GW190814 events to constrain deviation from GR.

In this article, we attempt to perform the ‘higher modes consistency’ test as proposed in Refs. [1, 2] on GW190814 with a focus on testing the validity of ‘no-hair theorem’ (or, in other words, the multi-polar structure of radiation as expected in GR) and quantify its evidence against scenarios favoring possible violations. We note that the efficiency of such test may also be dependent on the accuracy of models for gravitational radiation being used. Different gravitational waveform models employ different modeling strategies and have varying degree of accuracy when compared to numerical relativity (NR) data. These models mostly fall in three different categories: effective-one-body (EOB) waveform family [76–80], phenomenological (Phenom) waveform family [81–86], and NR based surrogate waveforms [87–89]. To understand how waveform systematic may affect the test accuracy, we use four different waveform models in our analysis. We also investigate the effects of the availability of different higher order modes. While numerous studies have focused in understanding possible biases in usual parameter inference of the detected GW signals due to not including higher order modes [90–101], such exercises have rarely been taken up for null-tests of GR like the ‘higher modes consistency’ test [102].

The rest of the paper is organized as follows. Section II presents a brief outline of the higher modes consistency test and Section III describes the data analysis framework including Bayesian inference. In Section IV, we perform the higher modes consistency test on GW190814 strain data using different waveform models and modes content. We then quantify the evidence for the ‘no-hair theorem’ in GR by computing Bayes factors. In this section, we also investigate the effects of higher order harmonics by employing different combination of the higher modes. We show that including only select higher order modes may lead to false identification of a departure from the ‘no-hair theorem’ if the detector sensitivity improves by almost an order of magnitude. Finally, in Section V, we summarize our results and discuss the implications of our findings.

## II. HIGHER MODES CONSISTENCY TEST

### A. Gravitational radiation in GR

Gravitational radiation from the coalescence of a binary black hole in GR is usually written as a linear combination of two independent polarizations (‘plus’ and ‘cross’):

$$h_{\text{GR}}(t; t_c, \mathbf{n}, \boldsymbol{\lambda}) = h_{+, \text{GR}}(t; t_c, \mathbf{n}, \boldsymbol{\lambda}) - i h_{\times, \text{GR}}(t; t_c, \mathbf{n}, \boldsymbol{\lambda}), \quad (1)$$

where  $t_c$  is time at coalescence. This radiation can further be decomposed into a basis of  $-2$  spin-weighted spherical harmonics  $Y_{\ell m}^{-2}$  [103]:

$$h_{\text{GR}}(t; t_c, \mathbf{n}, \boldsymbol{\lambda}) = \frac{1}{d_L} \sum_{\ell=2}^{\infty} \sum_{m=-\ell}^{\ell} Y_{\ell m}^{-2}(\mathbf{n}) \hat{h}_{\ell m}(t; t_c, \boldsymbol{\lambda}), \quad (2)$$

The set of two angles  $\mathbf{n} = \{\iota, \varphi_0\}$  denotes the direction of radiation in the source frame:  $\iota$  is the inclination angle between the orbital angular momentum of the binary and line-of-sight to the observer and  $\varphi_c$  is the azimuthal angle at coalescence. The vector  $\boldsymbol{\lambda} := \{\mathcal{M}_c, q, \chi_1, \chi_2, \theta_1, \theta_2, \phi_{12}, \phi_{j1}\}$  are the intrinsic parameters that describe the binary: the chirp mass  $\mathcal{M}_c$ , mass ratio  $q$ , dimensionless spin magnitudes  $\chi_1$  and  $\chi_2$ , and four angles  $\{\theta_1, \theta_2, \phi_{12}, \phi_{j1}\}$  describing the spin orientation (cf. Appendix of [104] for definitions of these angles). Luminosity distance of the binary from the observer is  $d_L$ . So far, all GW detections of BBHs are consistent with signals emitted from quasicircular binaries. We, therefore, ignore eccentricity in our analysis.

Finally, the gravitational signal  $h(t)$  detected by interferometers is a linear combination of the plus and cross polarization of the radiation weighted by the antenna pattern functions of the GW detector  $F_+$  and  $F_{\times}$ :

$$h_{\text{GR}}(t; \theta_{\text{GR}}) = F_+(\alpha, \delta, \psi) h_{+, \text{GR}}(t; t_c, \mathbf{n}, \boldsymbol{\lambda}) + F_{\times}(\alpha, \delta, \psi) h_{\times, \text{GR}}(t; t_c, \mathbf{n}, \boldsymbol{\lambda}), \quad (3)$$

where right ascension  $\alpha$  and declination  $\delta$  are the sky localization angles and  $\psi$  is the polarization angle. Together, this set of 15 parameters  $\theta_{\text{GR}} := \{t_c, \varphi_0, \iota, d_L, \alpha, \delta, \psi, \boldsymbol{\lambda}\}$  describes a gravitational wave signal for binary black hole merger in GR.

### B. Formulation of the higher modes consistency test

For quasi-circular binaries in GR, the set of *intrinsic* parameters  $\boldsymbol{\lambda}$  i.e., the masses and spins of the two black holes uniquely determines each of the spherical harmonic modes,  $\hat{h}_{\ell m}(t; t_c, \boldsymbol{\lambda})$ . The consistency of different spherical harmonic modes of the radiation provides a unique test of the ‘no-hair’ nature of binary black holes in GR. This involves estimating the intrinsic parameters of the binary from different spherical harmonic modes of the radiation and checking their consistency. Inconsistency between different spherical harmonic modes would indicate a departure from the multipolar structure of the radiation as expected from a binary black hole system in GR. This, however, requires that different spherical harmonics modes have sufficient signal-to-noise ratios so that they can be well resolved.

Alternatively, one can look for consistencies between the dominant  $(\ell, m) = (2, \pm 2)$  mode of the gravitational radiation, and the sub-dominant modes. Following [1, 2], we allow inconsistencies between the intrinsic parameters estimated from the dominant mode and the higher order modes by introducing a set of deviation parameters for masses in the higher modes:

$$\Delta \boldsymbol{\lambda} := \{\Delta \mathcal{M}_c, \Delta q\}. \quad (4)$$

Gravitational radiation then reads:

$$\begin{aligned} h_{\text{nonGR}}(t; t_c, \mathbf{n}, \boldsymbol{\lambda}, \Delta\boldsymbol{\lambda}) = & \sum_{m=\pm 2} Y_{2m}^{-2}(\mathbf{n}) h_{2m}(t, \boldsymbol{\lambda}) \\ & + \sum_{\text{HM}} Y_{\ell m}^{-2}(\mathbf{n}) h_{\ell m}(t, \boldsymbol{\lambda}, \Delta\boldsymbol{\lambda}). \end{aligned} \quad (5)$$

Here, HM indicates sum over higher order modes i.e. all modes other than  $(\ell, m) = (2, \pm 2)$ . In terms of the ‘plus’ and ‘cross’ polarizations this simply becomes:

$$\begin{aligned} h_{\text{nonGR}}(t; t_c, \mathbf{n}, \boldsymbol{\lambda}, \Delta\boldsymbol{\lambda}) = & h_{+, \text{nonGR}}(t; t_c, \mathbf{n}, \boldsymbol{\lambda}, \Delta\boldsymbol{\lambda}) \\ & - i h_{\times, \text{nonGR}}(t; t_c, \mathbf{n}, \boldsymbol{\lambda}, \Delta\boldsymbol{\lambda}). \end{aligned} \quad (6)$$

The test therefore have a set of 17 parameters to describe the signal:  $\theta_{\text{nonGR}} = \{\theta_{\text{GR}}, \Delta\boldsymbol{\lambda}\}$ . For GW signals produced by binary black hole mergers in GR, these additional parameters will be consistent with zero:  $\Delta\boldsymbol{\lambda} = \{0, 0\}$ . If the signal is not consistent with that produced by a BBH in GR,  $\Delta\boldsymbol{\lambda}$  will have non-zero values.

### III. DATA ANALYSIS FRAMEWORK

We now provide an executive summary of the data analysis framework used to perform the higher modes consistency test on GW190814.

#### A. Bayesian Inference

The measured strain data in a GW detector,

$$d(t) = h(t; \theta) + n(t), \quad (7)$$

is assumed to be a sum of the true signal,  $h(t; \theta)$ , and random Gaussian and stationary noise,  $n(t)$  with zero mean and a power spectral density (PSD),  $S_n(f)$ . Here,  $\theta$  is the set of parameters that describes the BBH signal that is embedded in the data. Given the time-series data  $d(t)$  and a model for GW signal  $H$  (i.e. whether the signal is consistent with binaries in GR or not), we use Bayes’ theorem to compute the *posterior probability distribution* (PDF) of the binary parameters,

$$p(\theta|d, H) = \frac{\pi(\theta|H)\mathcal{L}(d|\theta, H)}{\mathcal{Z}(d|H)}, \quad (8)$$

where  $\pi(\theta|H)$  is the *prior* astrophysical information of the probability distributions of BBH parameters  $\theta$  and  $\mathcal{L}(d|\theta, H)$  is the likelihood function describing how well each set of  $\theta$  matches the assumptions of the data.  $\mathcal{Z}(d|H)$  is called the model evidence or marginalized likelihood. For binaries in GR, we replace  $h(t; \theta)$  with  $h(t; \theta_{\text{GR}})$  (and  $\theta$  with the 15-dimensional set of parameters  $\theta_{\text{GR}}$ ) whereas, while performing the higher modes consistency test, we use  $h(t; \theta) = h(t; \theta_{\text{nonGR}})$  (and  $\theta = \{\theta_{\text{GR}}, \Delta\boldsymbol{\lambda}\}$ ). We also compute Bayes factors [105] in favor of the GR hypothesis

$$\mathcal{B} = \frac{\mathcal{Z}_{\text{GR}}}{\mathcal{Z}_{\text{nonGR}}}, \quad (9)$$

where  $\mathcal{Z}_{\text{GR}}$  and  $\mathcal{Z}_{\text{nonGR}}$  denote the evidence for a signal that is consistent with the multipolar structure as expected for a binary black hole in GR and signal that deviates from the expected behavior in GR respectively. The Bayes factor quantifies how much more likely that the data is described by a signal consistent with the ‘no-hair’ theorem in GR.

#### B. Setup

To compute the posterior probability distribution of BBH parameters  $p(\theta|d, H)$ , we use the Bayesian inference package `parallel-bilby` [104, 106, 107] with `dynesty` [108] sampler. We obtain the GW190814 strain and PSD data for all three detectors (LIGO-Hanford, LIGO-Livingston and Virgo) from the Gravitational Wave Open Science Center [3, 109]. The PSDs for these data were computed through the on-source `BayesWave` method [110–112], and use the inferred median PSDs in our analysis following the same assumptions as in Ref. [3]. Following the LVC analysis of the event, we start our data analysis at 20Hz for LIGO-Hanford and Virgo detectors. For LIGO Livingston, we use a minimum frequency of 30Hz [3].

To generate gravitational waveforms in GR, we use four different waveform models: `IMRPhenomXPHM` [113] (a state-of-art precessing spin multipolar gravitational waveform model), `IMRPhenomXHM` [114, 115] (a state-of-art multipolar gravitational waveform model for aligned spin binaries), `SEOBNRv4_ROM` [116] (a reduced order based effective-one-body model for aligned spin binaries) and `IMRPhenomHM` [117] (first multipolar gravitational waveform model for aligned spin binaries). While we use `IMRPhenomXPHM` as our *default* choice of waveform model, additional models have been used to understand waveform systematic (if any). In all cases, waveforms have been computed using `LALSuite` software library [118]. To generate waveforms with generic deviations from GR, we then modify `IMRPhenomXPHM`, `IMRPhenomXHM`, `IMRPhenomHM` and `SEONNRv4HM_ROM` waveforms following Eq.(5). For comparison, we also employ `IMRPhenomPv3HM` [86] (another multipolar gravitational waveform model for precessing spin binaries) as this model has been widely used to estimate the source properties of all LVC events.

#### C. Choice of priors

Our assumptions for the prior PDFs are mostly identical to the LVC analysis of GW190814 [3].

- i) We choose uniform priors for the chirp mass and mass ratio ( $5M_{\odot} \leq \mathcal{M}_c \leq 100M_{\odot}$  and  $4 \leq q \leq 20$ ), as defined in the rest frame of the Earth. The higher value ( $q = 4$ ) chosen for the lower limit of mass ratio prior does not affect our result as the resulting  $q$  posterior does not have any support for values  $q < 4$ . This is done in order for us to use a wider prior for the deviation parameters  $\Delta\mathcal{M}_c$  and  $\Delta q$ .

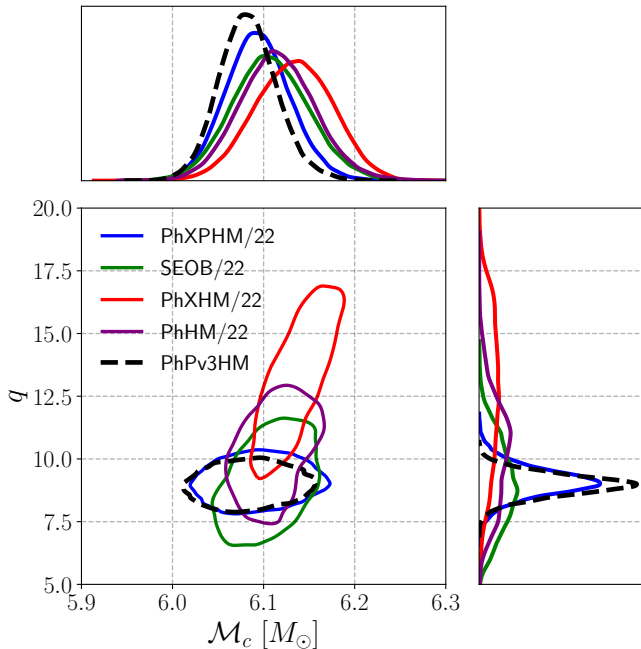


FIG. 1. Comparison of chirp mass  $\mathcal{M}_c$  and mass ratio  $q$  posteriors inferred from the  $(\ell, m) = (2, \pm 2)$  modes of the GW190814 strain data using four different waveform models: IMRPhenomXPHM (blue; labeled as PhXPHM), IMRPhenomXHM (red; labeled as PhXHM), IMRPhenomHM (magenta; labeled as PhHM) and SEONNRv4HM\_ROM (green; labeled as SEOB). We show the estimated two-dimensional contours for 90% confidence interval (middle panel) and one-dimensional kernel density estimates (KDEs) using Gaussian kernel (side panels). For comparison, we also show the estimates using all available modes in IMRPhenomPv3HM (black dashed line; labeled as PhPv3HM) model. Details are in Section IV A.

- ii) Uniform priors are also used for the component dimensionless spins ( $0.0 \leq \chi_1 \leq 1.0$  and  $0.0 \leq \chi_2 \leq 1.0$ ), with spin-orientations taken as uniform on the unit sphere.
- iii) The prior on the luminosity distance is taken such that it is uniform in co-moving volume [106] with  $1 \text{ Mpc} \leq D_L \leq 2000 \text{ Mpc}$ .
- iv) For the orbital inclination angle  $\theta_{JN}$ , we assume a uniform prior over  $0 \leq \cos \theta_{JN} \leq 1$ .
- v) Priors on the sky location parameters  $\alpha, \delta$  (right ascension and declination) are assumed to be uniform over the sky with periodic boundary conditions.
- vi) Finally, for the deviation parameters: we use uniform priors over  $-3M_\odot \leq \Delta\mathcal{M}_c \leq 3M_\odot$  and  $-3 \leq \Delta q \leq 3$ .

#### IV. RESULTS

We now investigate how well the deviation parameters can be measured from GW190814 strain data and discuss the implication of our findings on the validity of ‘no-hair’ theorem

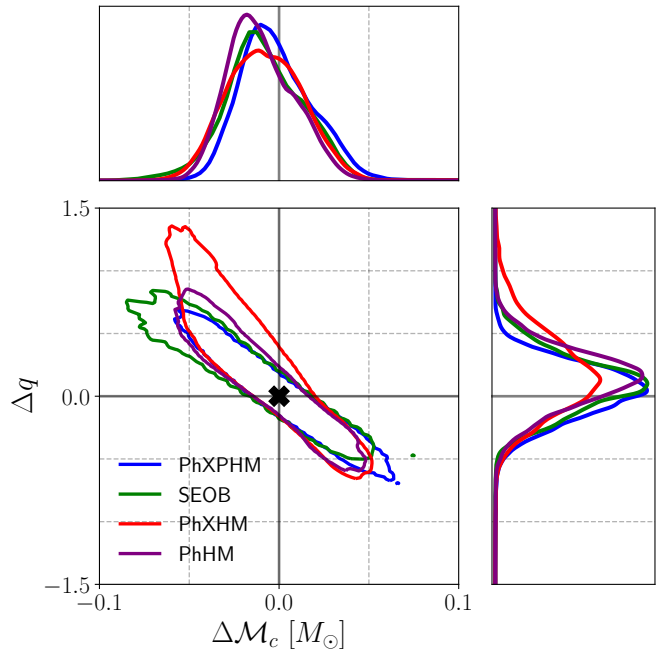


FIG. 2. Comparison of the posteriors of the deviation parameters  $\Delta\mathcal{M}_c$  and  $\Delta q$  inferred from GW190814 strain data using four different waveform models: IMRPhenomXPHM (blue; labeled as PhXPHM), IMRPhenomXHM (red; labeled as PhXHM), IMRPhenomHM (magenta; labeled as PhHM) and SEONNRv4HM\_ROM (green; labeled as SEOB). We show the estimated two-dimensional contours for 90% confidence interval (middle panel) and one-dimensional kernel density estimates (KDEs) using Gaussian kernel (side panels). The posteriors are fully consistent with the GR prediction of  $\Delta\mathcal{M}_c = \Delta q = 0$  (shown by a “+” sign in the center panel and by thin black lines in all panels). Details are in Section IV A.

for binary black holes in GR. Posteriors of select parameters of interest are also shown.

##### A. Constraining the deviation parameter

We perform the higher modes consistency tests on the detected GW190814 strain data using four different waveform models: IMRPhenomXPHM, IMRPhenomXHM, IMRPhenomHM and SEONNRv4HM\_ROM. While IMRPhenomXPHM is a precessing spin model, all remaining models are restricted to aligned-spin systems. The published LVC analysis [3], however, implies that GW190814 is a low-spinning system with effective inspiral spin  $\chi_{\text{eff}} = -0.001^{+0.060}_{-0.061}$  and an effective precession parameter  $\chi_p \leq 0.07$ . The aligned-spin models are, therefore, expected to capture the binary properties reasonably well. Employing different waveform models with varying modelling strategies will help us to identify any waveform systematic (if any) that may affect the accuracy of the higher modes consistency test particularly in the context of GW190814.

Higher modes consistency test simultaneously estimates the chirp mass  $\mathcal{M}_c$  and mass ratio  $q$  from the dominant  $(\ell, m) = (2, \pm 2)$  modes and the deviation parameters  $\Delta\mathcal{M}_c$



Waveform model	Available HOM
IMRPhenomXPHM	(2, ±1), (3, ±2), (3, ±3), (4, ±4)
IMRPhenomXHM	(2, ±1), (3, ±2), (3, ±3), (4, ±4)
IMRPhenomHM	(2, ±1), (3, ±2), (3, ±3), (4, ±3), (4, ±4)
SEOBNRv4_ROM	(2, ±1), (3, ±3), (4, ±4), (5, ±5)

TABLE I. Available higher order modes i.e. modes apart from the dominant  $(\ell, m) = (2, \pm 2)$  mode in various waveform models used in this study.

and  $\Delta q$  from the available higher order modes along with other parameters. Fig. 1 shows the inferred chirp mass  $\mathcal{M}_c$  and mass ratio  $q$  as estimated from the  $(2, \pm 2)$  modes using various waveform models. We show both the marginalized one-dimensional kernel density estimates (KDEs) using Gaussian kernel (side panels) and two-dimensional contours for 90% confidence intervals (middle panel). For comparison, we also show the inferred values estimated using *all* available modes in IMRPhenomPv3HM model (black dashed lines). We note that the  $(\ell, m) = (2, \pm 2)$  mode IMRPhenomXPHM estimates of  $\mathcal{M}_c$  and  $q$  matches IMRPhenomPv3HM estimates using *all* available modes. Aligned spin models, on the other hand, yield broader posteriors (and contours). However, these estimates do overlap with each other implying that the broadening of posteriors is due to the loss of information as these models assume the binaries to have aligned spin components only.

Constraints on the deviation parameters  $\Delta\mathcal{M}_c$  and  $\Delta q$  in the higher order modes (obtained using different waveform models) are shown in Fig. 2. We find that the deviation parameters are consistent with the GR values: a zero deviation is within the 90% credible interval across waveform models. It is interesting to note that, even though the  $(\ell, m) = (2, \pm 2)$  mode estimates of  $\mathcal{M}_c$  and  $q$  obtained from different waveform models (mostly between the estimates inferred with a precessing model and aligned spin models) have some noticeable differences, the posteriors for deviation parameters agree quite well to each other. The only exception is IMRPhenomXHM which prefers a longer tail for  $\Delta q$  (and for  $q$  too). In all cases, the fractional deviation  $\frac{\Delta\mathcal{M}_c}{\mathcal{M}_c}(\%)$  and  $\frac{\Delta q}{q}(\%)$  are only a few percent.

This exercise provides interesting insights into the waveform systematic. Various waveform models employed here include different higher order harmonics (see Table I). However, no significant biases in  $\Delta\mathcal{M}_c$  and  $\Delta q$  across waveform models (except IMRPhenomXHM) implies that, even though there are differences in  $\mathcal{M}_c$  and  $q$  estimates across different models, inferred values from the  $(2, \pm 2)$  and higher order modes for a particular waveform model is consistent with each other.

## B. Testing the ‘no-hair’ theorem

Next, we test the ‘no-hair’ hypothesis and quantify its evidence in data. This is done in two steps. First, we analyze the data assuming a GR hypothesis: this involves estimating the set of 15 parameters in GR that describes the signal. Then, we repeat the analysis with a non-GR hypothesis where the signal

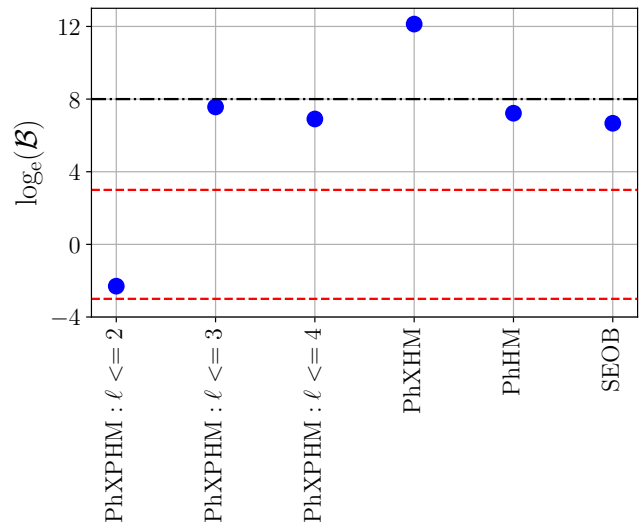


FIG. 3.  $\log_e(\mathcal{B})$  in favor of the hypothesis that the observed strain data is consistent with the multipolar structure expected for signals emitted from binary black holes in GR.  $\log_e(\mathcal{B}) = 0$  indicates both the GR and deviation from binary in GR hypothesis are equally likely. To put things into perspective, we also show  $\log_e(\mathcal{B}) = \pm 3$  (which provides enough hint for a hypothesis) and  $\log_e(\mathcal{B}) = \pm 8$  (which strongly favors a hypothesis). Details are in Section IV B.

is modified according to Eq.(6) to allow possible departure from the multi-polar structure of gravitational radiation in GR. We then compute the Bayes factor in favor of the ‘no-hair’ theorem. In Fig. 3, we show the estimated Bayes factors (in logarithmic scale) for the ‘no-hair’ hypothesis in GR estimated using different waveform models. To put things into perspective, a  $\log_e(\mathcal{B}) = 0$  indicates that both the ‘no-hair’ hypothesis in GR and the hypothesis supporting a deviation from it are equally likely while  $\log_e(\mathcal{B}) = \pm 3$  ( $\log_e(\mathcal{B}) = \pm 8$ ) implies some support for a particular hypothesis (implies that the data strongly favors a particular hypothesis). For all of the waveform models, we find that the data has overwhelming support the ‘no-hair’ hypothesis with  $\log_e(\mathcal{B}) \sim 7 - 8$ . Therefore, our study suggests that the data favors the GR hypothesis where this deviation parameters are set to zero.

## C. Effects of higher order modes

We now investigate how the mode contents in the higher order harmonics affect the test accuracy. We demonstrate the effect of higher order modes using our default choice of waveform model IMRPhenomXPHM. To do this, we perform the higher modes consistency test with different combination of modes:

- First, we only include the  $(\ell, m) = (2, \pm 1)$  modes in our higher harmonics.
- More modes are then gradually included. We repeat the exercise with another two configurations of mode content: (i)  $\{(2, \pm 1), (3, \pm 2), (3, \pm 3)\}$  (including

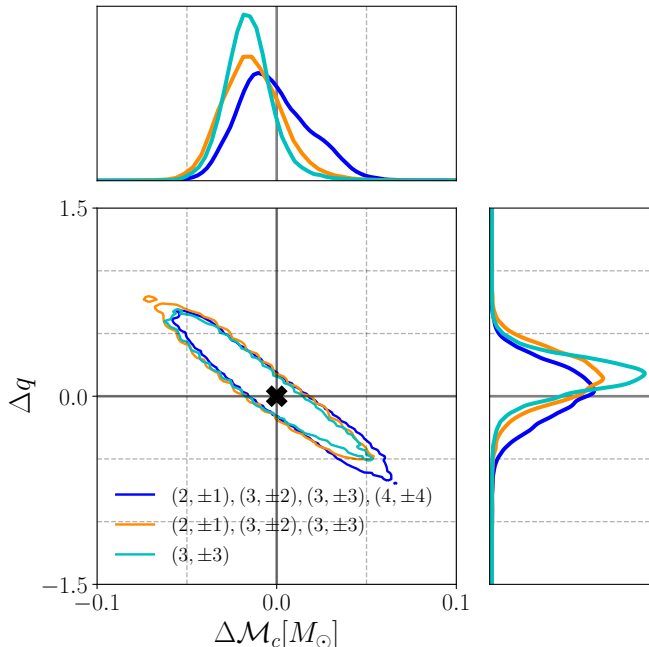


FIG. 4. Comparison of the posteriors of the deviation parameters  $\Delta\mathcal{M}_c$  and  $\Delta q$  inferred from GW190814 strain data using different mode content in the higher order modes: (i)  $(\ell, m) = \{(2, \pm 1), (3, \pm 2), (3, \pm 3), (4, \pm 4)\}$  (blue), (ii)  $(\ell, m) = \{(2, \pm 1), (3, \pm 2), (3, \pm 3)\}$  (orange) and (iii)  $(\ell, m) = \{(3, \pm 3)\}$  (cyan). We show the estimated two-dimensional contours for 90% confidence intervals (middle panel) and one-dimensional kernel density estimates (KDEs) using Gaussian kernel (side panels). The posteriors are fully consistent with the GR prediction of  $\Delta\mathcal{M}_c = \Delta q = 0$  (shown by a “+” sign in the center panel and by thin black lines in all panels). Details are in Section IV C.

all available  $\ell \leq 3$  modes in IMRPhenomXPHM); and (ii)  $\{(2, \pm 1), (3, \pm 2), (3, \pm 3), (4, \pm 4)\}$  (including all available  $\ell \leq 4$  modes in IMRPhenomXPHM).

- Finally, we note that the LVC analysis finds strong support for the  $(\ell, m) = (3, \pm 3)$  modes in the strain data apart from the dominant  $(\ell, m) = (2, \pm 2)$  modes [3]. We, therefore, redo our analysis for the case where the higher harmonics only include the  $(\ell, m) = (3, \pm 3)$  mode.

Fig. 3 shows the recovered Bayes factors in support of the GR hypothesis for varying mode content. Interestingly, we observe that for the case when *only*  $(\ell, m) = (2, \pm 1)$  modes are included in the higher harmonics, the deviation parameters remains mostly unresolved (not shown) and the test favors ( $\log_e(\mathcal{B}) \sim -3.5$ ) the hypothesis that the data is better described by a departure from the multi-polar structure in radiation as expected in GR. However, as we include other important modes, specially  $(\ell, m) = (3, \pm 3)$  modes,  $\log_e(\mathcal{B})$  becomes positive again implying increased support for the GR hypothesis. In Fig. 4, we show the posteriors for the deviation parameters  $\Delta\mathcal{M}_c$  and  $\Delta q$ . We notice that even though the posteriors are all consistent with GR expectation of zero, they show an interesting trend. Both  $\Delta\mathcal{M}_c$  and  $\Delta q$  has sharper peaks when they

are estimated from only the  $(\ell, m) = (3, \pm 3)$  modes. Furthermore, the peaks appear to be shifted from zero even though the posteriors are still consistent with zero at 90% credible intervals. As we include more and more modes, the posteriors becomes broader but the peaks shift towards zero. This study clearly shows the need to have as many higher order modes as possible so that not only our usual PE estimates are correct, but also any tests of GR, specially higher modes consistency tests or quasi-normal modes consistency tests, are able to provide trustful results.

#### D. Nature of the compact objects

To test our null hypothesis that GW190814 signal is produced by a BBH in GR, we constrain the deviation parameters  $\Delta\mathcal{M}_c$  and  $\Delta q$ . For BBH signal in GR, these deviation parameters are expected to be consistent with zero. Non-zero values  $\Delta\mathcal{M}_c$  and  $\Delta q$  would imply a possible departure from a BBH in GR. Such departures would point to either (i) a violation of GR; or (ii) a merger of compact objects that are not black holes such as neutron stars or other exotic objects; or (iii) the possibility that the signal might have been modified due to other astrophysical processes (such as environmental effects or lensing) that have been neglected in analysis. We point out that the higher modes consistency test can distinguish a NSBH signal from a BBH when the signal-to-noise ratio is high (cf. Fig. 11 of Ref. [1]). Overall, our results in Section IV B favors the hypothesis that the GW signal from GW190814 is consistent with the multipolar structure of radiation expected from a binary black hole merger in GR over possible departure from it by  $\log_e(\mathcal{B}) \sim 7 - 8$ . However, we must caution that it is still possible that the signal have imprints of beyond GR effects or signature of compact objects apart from BBH; and those imprints may be small enough that they have not been captured by this test in the current signal-to-noise ratio.

#### E. Implications for future detectors with improved sensitivity

Our findings in Section IV C suggests that any higher modes consistency tests using only select higher order harmonics may falsely identify a GR signal if the signal has high SNRs. Such scenarios may occur as our detectors gradually become more sensitive. We investigate this possibility using a simplistic approach that fits in between a real GW data analysis and a simulated data analysis. We decide to use the actual strain and calibration data for GW190814 but re-scale the PSD by some factor to simulate the same event but in a more sensitive network of detectors. We consider two different cases where the PSDs across detectors have been re-scaled by a factor of  $\frac{1}{7.5}$  and  $\frac{1}{12.5}$  apart from the case where we use actual PSDs. We then perform the higher modes consistency tests employing IMRPhenomXPHM model. Furthermore, we use only  $(\ell, m) = (3, \pm 3)$  modes in the higher harmonics. While we could have included all the available modes in the model, our choice is motivated by the findings that when only  $(\ell, m) = (3, \pm 3)$  modes are included in the higher harmonics, both  $\Delta\mathcal{M}_c$  and  $\Delta q$

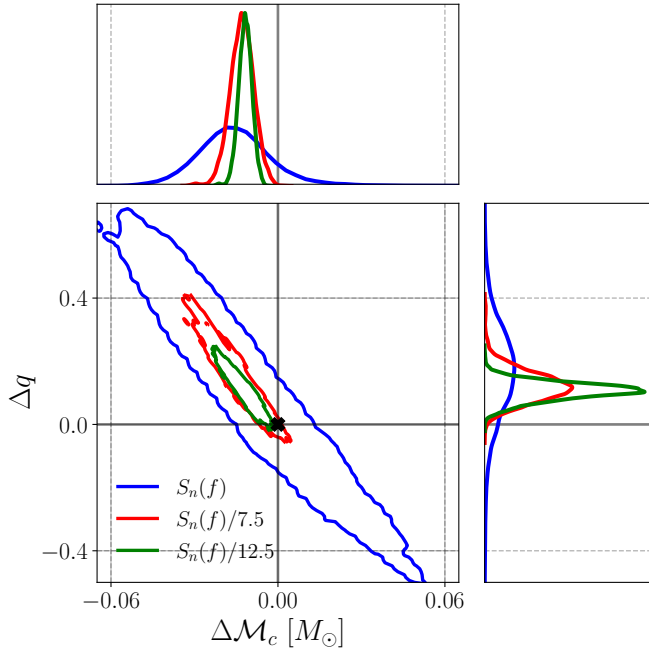


FIG. 5. Comparison of the posteriors of the deviation parameters  $\Delta\mathcal{M}_c$  and  $\Delta q$  inferred from GW190814 strain data employing IMRPhenomXPHM model (only the  $(\ell, m) = (3, \pm 3)$  modes are included in the higher harmonics) with rescaled PSDs for all three detectors to imitate a future network of detectors with improved sensitivity. Apart from the results obtained using the actual PSDs (blue), we show results inferred from two other cases where the PSDs across detectors have been scaled by a factor of  $1/7.5$  (red) and  $1/12.5$  (green). We show the estimated two-dimensional contours for 90% confidence intervals (middle panel) and one-dimensional kernel density estimates (KDEs) using Gaussian kernel (side panels). GR prediction of  $\Delta\mathcal{M}_c = \Delta q = 0$  is shown by a “+” sign in the center panel and by thin black lines in all panels. When the PSDs are rescaled by a factor of  $1/7.5$ , resultant posteriors become inconsistent with GR. Details are in Section IV E.

have sharper peaks that are slightly offset from zeros (Fig. 4). We find that, due to the improvement in sensitivity,  $\Delta\mathcal{M}_c$  and  $\Delta q$  posteriors become sharper as expected when the PSDs are scaled. Interestingly, for the case where the PSDs have been scaled by a factor of  $\frac{1}{12.5}$ , higher modes consistency test yields  $\Delta\mathcal{M}_c$  and  $\Delta q$  posteriors that are inconsistent with GR. We must mention that the exercise of rescaling the PSDs may exaggerate the effect of the noise that is on top of the signal and may bias the parameter estimation. Nonetheless, this demonstrates that future models need to include more higher order modes to avoid scenarios where a purely GR signal may be labeled as a violation of GR as a result of the loss of information due to the unavailability of many higher order harmonics.

## V. FINAL REMARKS

We provide a comprehensive analysis of the evidence for ‘no-hair’ theorem for BBH in GR using GW190814 strain data. To test the validity of the ‘no-hair’ theorem in GR, we per-

form ‘higher modes consistency’ test proposed in Refs. [1, 2]. The test checks whether the estimation of chirp mass  $\mathcal{M}_c$  and mass ratio  $q$  from the dominant quadrupolar  $(\ell, m) = (2, \pm 2)$  modes are consistent with values inferred from the higher order harmonics. This is done by introducing additional deviation parameters in masses for the higher order modes:  $\Delta\mathcal{M}_c$  and  $\Delta q$ . If the signal is originated from a binary black hole system as described in GR, these two deviation parameters will be zero. A non-zero value will point to possible modifications of gravity or astrophysical phenomenon not considered in analysis or even exotic nature of the compact objects. To detect (or nullify) any possible biases in inferred  $\Delta\mathcal{M}_c$  and  $\Delta q$  parameters originating from the choice of waveform models, we perform the test using four different models having varying mode contents and accuracy: IMRPhenomXPHM, IMRPhenomXHM, IMRPhenomHM and SEONNRv4HM\_ROM. These models also have different domain of validity. While IMRPhenomXPHM models GW signal from generically spinning binaries, all other models are restricted to only aligned-spin binary black holes. As the detected binary has negligible spin, these models are expected to describe the system reasonably well.

We find that the deviation parameters  $\Delta\mathcal{M}_c$  and  $\Delta q$  are broadly consistent with zeros irrespective of the waveform model used (Fig. 2). We note that similar test have recently been applied to GW190412 and GW190814 strain data [74]. The test includes only  $(2, \pm 2)$  and  $(3, \pm 3)$  modes in their study and considers two different ways to look for the consistency: (i) by allowing all intrinsic parameters including spins to assume different values in different modes; and (ii) then allowing only the masses to have different values across modes. In both the cases, orbital phases are free to have different values in  $(2, \pm 2)$  and  $(3, \pm 3)$  modes. In Fig. 6, we compare results obtained using the later strategy in Ref. [74] against that of ours obtained using (i) all available higher order modes in the waveform model and (ii) using only  $(\ell, m) = \{(3, \pm 3)\}$  mode in the higher harmonics. We find that while  $\Delta\mathcal{M}_c$  and  $\Delta q$  posteriors have visible differences, all three posteriors are consistent with GR expectation and the fractional deviations  $\frac{\Delta\mathcal{M}_c}{\mathcal{M}_c}(\%)$  and  $\frac{\Delta q}{q}(\%)$  are only a few percent in all cases. We attribute the remaining differences to the differences in the formulation of the consistency tests. For example, we do not allow the orbital phase to take different values in different modes.

GW190814 data overwhelmingly supports the hypothesis that the signal obeys the ‘no-hair theorem’ in GR (i.e. the signal is consistent with the multipolar structure of radiation as expected from a merging binary black hole in GR) over hypothesis proposing a deviation from the ‘no-hair theorem’ (Fig. 3). The log Bayes factor computed in favor of the ‘no-hair theorem’ is found to be  $\log_c(\mathcal{B}) \sim 7 - 8$ . This implies that the binary is likely to be a binary black hole in GR. We must caution that it is, however, possible that the a binary is not a BBH or the signal actually obeys a theory of gravity different from GR but the test is unable to pick up those signatures at the current signal-to-noise.

We further show that including several higher order modes are crucial for consistency tests like this one. We observe that when the higher harmonics only include the  $(\ell, m) = (2, \pm 1)$  modes, the test favors a violation of GR even though the de-

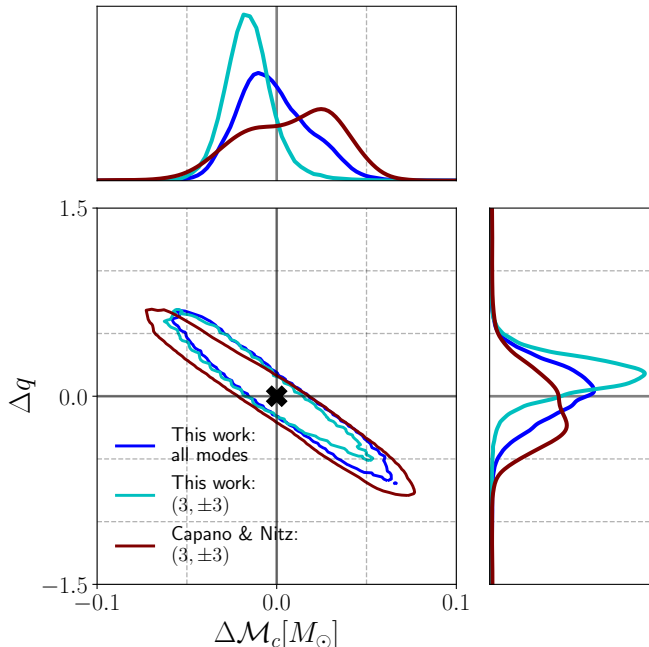


FIG. 6. Comparison of the posteriors of the deviation parameters  $\Delta M_c$  and  $\Delta q$  inferred using our higher modes consistency test [1, 2] and results obtained in Ref. [74]. We show our  $\Delta M_c$  and  $\Delta q$  estimates using (i) all available higher order modes in the waveform model (blue) and (ii) using only  $(\ell, m) = \{(3, \pm 3)\}$  mode in the higher harmonics (cyan). Results obtained in Ref [74] using only the  $(\ell, m) = \{(3, \pm 3)\}$  mode in the higher harmonics through a different version of the higher modes consistency test is shown in brown. We show the estimated two-dimensional contours for 90% confidence intervals (middle panel) and one-dimensional kernel density estimates (KDEs) using Gaussian kernel (side panels). The posteriors are fully consistent with the GR prediction of  $\Delta M_c = \Delta q = 0$  (shown by a “+” sign in the center panel and by thin black lines in all panels). Details are in Section V.

viation parameters are mostly unresolved (Fig. 3). This is due to the inability of the waveform model to account for neglected higher order modes like  $(\ell, m) = (3, \pm 3)$  modes. Similar results have previously been obtained for cases where the higher-order modes are present in the simulated GR signal but the recovery template used to test GR includes only dominant  $(2, \pm 2)$  modes [119]. Next, we also show that while having only  $(\ell, m) = (3, \pm 3)$  modes in the higher harmonics would yield results consistent with GR expectation for current detectors (Fig. 4), it might not be enough when detector sensitivity improves in future. We demonstrate this by rescaling the PSDs by some constant factor and redoing the analysis. We find that when the sensitivity improves by at least a factor of  $\sim 12.5$ , this test triggers a false alarm if none of the higher harmonics apart from  $(\ell, m) = (3, \pm 3)$  modes are included (Fig. 5).

Apart from providing support for the ‘no-hair theorem’, our study therefore calls for having as many higher order modes as possible in anticipation of future improvements in GW detectors. Our study employs four different state-of-art

waveform models from only the Phenom and EOB families. As none of the existing NR surrogate waveform model covers mass ratio  $q \sim 10$  for spinning binaries, we have not been able to use it in our analysis. Works are, however, underway to build NR-based or NR-tuned perturbation theory based surrogate waveform models for high mass binaries with spins. Availability of such models having more spherical harmonic modes compared to the existing phenomenological and EOB models may further improve our ability to test the ‘no-hair’ theorem with detected GW signals. We leave that for future explorations.

## ACKNOWLEDGMENTS

T.I. thanks Vijay Varma, Scott Field, Gaurav Khanna, Max Isi, Harald Pfeiffer and Juan Calderon Bustillo for helpful feedback on the manuscript; Parameswaran Ajith, Ajit Kumar Mehta and Abhirup Ghosh for numerous discussion during the development of the test (cf. [1]); Carl-Johan Haster for some helps related to plotting and Rory Smith for his comments on Bayes factor computation. Simulations were performed on CARNiE at the Center for Scientific Computing and Visualization Research (CSCVR) of UMassD, which is supported by the ONR/DURIP Grant No. N00014181255 and the MIT Lincoln Labs *SuperCloud* GPU supercomputer supported by the Massachusetts Green High Performance Computing Center (MGHPCC). This research was supported in part by the Heising-Simons Foundation, the Simons Foundation, and National Science Foundation Grant No. NSF PHY-1748958. The author acknowledge support of NSF Grants No. PHY-1806665 and No. DMS-1912716.

This research has made use of data, software and/or web tools obtained from the Gravitational Wave Open Science Center (<https://www.gw-openscience.org/>) [120], a service of LIGO Laboratory, the LIGO Scientific Collaboration and the Virgo Collaboration. LIGO Laboratory and Advanced LIGO are funded by the United States National Science Foundation (NSF) as well as the Science and Technology Facilities Council (STFC) of the United Kingdom, the Max-Planck-Society (MPS), and the State of Niedersachsen/Germany for support of the construction of Advanced LIGO and construction and operation of the GEO600 detector. Additional support for Advanced LIGO was provided by the Australian Research Council. Virgo is funded, through the European Gravitational Observatory (EGO), by the French Centre National de Recherche Scientifique (CNRS), the Italian Istituto Nazionale di Fisica Nucleare (INFN) and the Dutch Nikhef, with contributions by institutions from Belgium, Germany, Greece, Hungary, Ireland, Japan, Monaco, Poland, Portugal, Spain. This is LIGO Document Number DCC-P2100392.

## REFERENCES



- [1] Tousif Islam, Ajit Kumar Mehta, Abhirup Ghosh, Vijay Varma, Parameswaran Ajith, and B. S. Sathyaprakash, “Testing the no-hair nature of binary black holes using the consistency of multipolar gravitational radiation,” *Phys. Rev. D* **101**, 024032 (2020), arXiv:1910.14259 [gr-qc].
- [2] Siddharth Dhanpal, Abhirup Ghosh, Ajit Kumar Mehta, Parameswaran Ajith, and B. S. Sathyaprakash, “A no-hair test for binary black holes,” *Phys. Rev. D* **99**, 104056 (2019), arXiv:1804.03297 [gr-qc].
- [3] R. Abbott *et al.* (LIGO Scientific, Virgo), “GW190814: Gravitational Waves from the Coalescence of a 23 Solar Mass Black Hole with a 2.6 Solar Mass Compact Object,” *Astrophys. J. Lett.* **896**, L44 (2020), arXiv:2006.12611 [astro-ph.HE].
- [4] R. Abbott *et al.* (LIGO Scientific, Virgo), “GWTC-2: Compact Binary Coalescences Observed by LIGO and Virgo During the First Half of the Third Observing Run,” *Phys. Rev. X* **11**, 021053 (2021), arXiv:2010.14527 [gr-qc].
- [5] J. Aasi *et al.* (LIGO Scientific), “Advanced LIGO,” *Class. Quant. Grav.* **32**, 074001 (2015), arXiv:1411.4547 [gr-qc].
- [6] F. Acernese *et al.* (VIRGO), “Advanced Virgo: a second-generation interferometric gravitational wave detector,” *Class. Quant. Grav.* **32**, 024001 (2015), arXiv:1408.3978 [gr-qc].
- [7] Charles D. Bailyn, Raj K. Jain, Paolo Coppi, and Jerome A. Orosz, “The mass distribution of stellar black holes,” *The Astrophysical Journal* **499**, 367–374 (1998).
- [8] Will M. Farr, Niharika Sravan, Andrew Cantrell, Laura Kreiberg, Charles D. Bailyn, Ilya Mandel, and Vicky Kalogera, “The Mass Distribution of Stellar-Mass Black Holes,” *Astrophys. J.* **741**, 103 (2011), arXiv:1011.1459 [astro-ph.GA].
- [9] Feryal Ozel, Dimitrios Psaltis, Ramesh Narayan, and Antonio Santos Villarreal, “On the Mass Distribution and Birth Masses of Neutron Stars,” *Astrophys. J.* **757**, 55 (2012), arXiv:1201.1006 [astro-ph.HE].
- [10] Feryal Ozel, Dimitrios Psaltis, Ramesh Narayan, and Jeffrey E. McClintock, “The Black Hole Mass Distribution in the Galaxy,” *Astrophys. J.* **725**, 1918–1927 (2010), arXiv:1006.2834 [astro-ph.GA].
- [11] V. P. Goncalves, J. C. Jimenez, and L. Lazzari, “Electrically charged supermassive twin stars,” (2021), arXiv:2109.04806 [hep-ph].
- [12] H. C. Das, Ankit Kumar, and S. K. Patra, “Dark matter admixed neutron star as a possible compact component in the GW190814 merger event,” *Phys. Rev. D* **104**, 063028 (2021), arXiv:2109.01853 [astro-ph.HE].
- [13] L. S. Rocha, R. R. A. Bachega, J. E. Horvath, and P. H. R. S. Moraes, “The maximum mass of neutron stars may be higher than expected: an inference from binary systems,” (2021), arXiv:2107.08822 [astro-ph.HE].
- [14] Antonios Nathanail, Elias R. Most, and Luciano Rezzolla, “GW170817 and GW190814: tension on the maximum mass,” *Astrophys. J. Lett.* **908**, L28 (2021), arXiv:2101.01735 [astro-ph.HE].
- [15] Bhaskar Biswas, Rana Nandi, Prasanta Char, Sukanta Bose, and Nikolaos Stergioulas, “GW190814: on the properties of the secondary component of the binary,” *Mon. Not. Roy. Astron. Soc.* **505**, 1600–1606 (2021), arXiv:2010.02090 [astro-ph.HE].
- [16] I. Bombaci, A. Drago, D. Logoteta, G. Pagliara, and I. Vidana, “Was GW190814 a Black Hole–Strange Quark Star System?” *Phys. Rev. Lett.* **126**, 162702 (2021), arXiv:2010.01509 [nucl-th].
- [17] Zheng Cao, Lie-Wen Chen, Peng-Cheng Chu, and Ying Zhou, “GW190814: Circumstantial Evidence for Up-Down Quark Star,” (2020), arXiv:2009.00942 [astro-ph.HE].
- [18] Rafael C. Nunes, Jaziel G. Coelho, and José C. N. de Araujo, “Weighing massive neutron star with screening gravity: a look on PSR J0740 + 6620 and GW190814 secondary component,” *Eur. Phys. J. C* **80**, 1115 (2020), arXiv:2008.10395 [astro-ph.HE].
- [19] Kaixuan Huang, Jinniu Hu, Ying Zhang, and Hong Shen, “The possibility of the secondary object in GW190814 as a neutron star,” *Astrophys. J.* **904**, 39 (2020), arXiv:2008.04491 [nucl-th].
- [20] V. Dexheimer, R. O. Gomes, T. Klähn, S. Han, and M. Salinas, “GW190814 as a massive rapidly rotating neutron star with exotic degrees of freedom,” *Phys. Rev. C* **103**, 025808 (2021), arXiv:2007.08493 [astro-ph.HE].
- [21] Sebastien Clesse and Juan Garcia-Bellido, “GW190425, GW190521 and GW190814: Three candidate mergers of primordial black holes from the QCD epoch,” (2020), arXiv:2007.06481 [astro-ph.CO].
- [22] Ingo Tews, Peter T. H. Pang, Tim Dietrich, Michael W. Coughlin, Sarah Antier, Mattia Bulla, Jack Heinzl, and Lina Issa, “On the Nature of GW190814 and Its Impact on the Understanding of Supranuclear Matter,” *Astrophys. J. Lett.* **908**, L1 (2021), arXiv:2007.06057 [astro-ph.HE].
- [23] Nai-Bo Zhang and Bao-An Li, “GW190814’s Secondary Component with Mass  $2.50\text{--}2.67 M_{\odot}$  as a Superfast Pulsar,” *Astrophys. J.* **902**, 38 (2020), arXiv:2007.02513 [astro-ph.HE].
- [24] Reed Essick and Philippe Landry, “Discriminating between Neutron Stars and Black Holes with Imperfect Knowledge of the Maximum Neutron Star Mass,” *Astrophys. J.* **904**, 80 (2020), arXiv:2007.01372 [astro-ph.HE].
- [25] Kyriakos Vattis, Isabelle S. Goldstein, and Savvas M. Koushiappas, “Could the  $2.6 M_{\odot}$  object in GW190814 be a primordial black hole?” *Phys. Rev. D* **102**, 061301 (2020), arXiv:2006.15675 [astro-ph.HE].
- [26] Tom Broadhurst, Jose M. Diego, and George F. Smoot, “Interpreting LIGO/Virgo ‘Mass-Gap’ events as lensed Neutron Star-Black Hole binaries,” (2020), arXiv:2006.13219 [astro-ph.CO].
- [27] Manuel Arca Sedda, “Dynamical Formation of the GW190814 Merger,” *Astrophys. J. Lett.* **908**, L38 (2021), arXiv:2102.03364 [astro-ph.HE].
- [28] Wenbin Lu, Paz Beniamini, and Clément Bonnerot, “On the formation of GW190814,” *Mon. Not. Roy. Astron. Soc.* **500**, 1817–1832 (2020), arXiv:2009.10082 [astro-ph.HE].
- [29] Bin Liu and Dong Lai, “Hierarchical Black-Hole Mergers in Multiple Systems: Constrain the Formation of GW190412, GW190814 and GW190521-like events,” *Mon. Not. Roy. Astron. Soc.* **502**, 2049–2064 (2021), arXiv:2009.10068 [astro-ph.HE].
- [30] Volodymyr Takhistov, George M. Fuller, and Alexander Kusenkov, “Test for the Origin of Solar Mass Black Holes,” *Phys. Rev. Lett.* **126**, 071101 (2021), arXiv:2008.12780 [astro-ph.HE].
- [31] Hai-Tian Wang, Shao-Peng Tang, Peng-Cheng Li, Ming-Zhe Han, and Yi-Zhong Fan, “Tight constraints on Einstein-dilation-Gauss-Bonnet gravity from GW190412 and GW190814,” *Phys. Rev. D* **104**, 024015 (2021).
- [32] Artyom V. Astashenok, Salvatore Capozziello, Sergei D. Odintsov, and Vasilis K. Oikonomou, “Extended Gravity Description for the GW190814 Supermassive Neutron Star,” *Phys. Lett. B* **811**, 135910 (2020), arXiv:2008.10884 [gr-qc].

- [33] J. W. Moffat, “Modified Gravity (MOG) and Heavy Neutron Star in Mass Gap,” (2020), [arXiv:2008.04404 \[gr-qc\]](#).
- [34] R. Abbott *et al.* (LIGO Scientific, Virgo), “Tests of general relativity with binary black holes from the second LIGO-Virgo gravitational-wave transient catalog,” *Phys. Rev. D* **103**, 122002 (2021), [arXiv:2010.14529 \[gr-qc\]](#).
- [35] N. V. Krishnendu, K. G. Arun, and Chandra Kant Mishra, “Testing the binary black hole nature of a compact binary coalescence,” *Phys. Rev. Lett.* **119**, 091101 (2017), [arXiv:1701.06318 \[gr-qc\]](#).
- [36] N. V. Krishnendu, M. Saleem, A. Samajdar, K. G. Arun, W. Del Pozzo, and Chandra Kant Mishra, “Constraints on the binary black hole nature of GW151226 and GW170608 from the measurement of spin-induced quadrupole moments,” *Phys. Rev. D* **100**, 104019 (2019), [arXiv:1908.02247 \[gr-qc\]](#).
- [37] Nathan K. Johnson-Mcdaniel, Arunava Mukherjee, Rahul Kashyap, Parameswaran Ajith, Walter Del Pozzo, and Salvatore Vitale, “Constraining black hole mimickers with gravitational wave observations,” *Phys. Rev. D* **102**, 123010 (2020), [arXiv:1804.08026 \[gr-qc\]](#).
- [38] Shilpa Kastha, Anuradha Gupta, K. G. Arun, B. S. Sathyaprakash, and Chris Van Den Broeck, “Testing the multipole structure of compact binaries using gravitational wave observations,” *Phys. Rev. D* **98**, 124033 (2018), [arXiv:1809.10465 \[gr-qc\]](#).
- [39] Shilpa Kastha, Anuradha Gupta, K. G. Arun, B. S. Sathyaprakash, and Chris Van Den Broeck, “Testing the multipole structure and conservative dynamics of compact binaries using gravitational wave observations: The spinning case,” *Phys. Rev. D* **100**, 044007 (2019), [arXiv:1905.07277 \[gr-qc\]](#).
- [40] Gregorio Carullo, Gunnar Riemenschneider, Ka Wa Tsang, Alessandro Nagar, and Walter Del Pozzo, “GW150914 peak frequency: a novel consistency test of strong-field General Relativity,” *Class. Quant. Grav.* **36**, 105009 (2019), [arXiv:1811.08744 \[gr-qc\]](#).
- [41] Gregorio Carullo, Walter Del Pozzo, and John Veitch, “Observational Black Hole Spectroscopy: A time-domain multimode analysis of GW150914,” *Phys. Rev. D* **99**, 123029 (2019), [Erratum: *Phys.Rev.D* 100, 089903 (2019)], [arXiv:1902.07527 \[gr-qc\]](#).
- [42] Gregorio Carullo, “Enhancing modified gravity detection from gravitational-wave observations using the parametrized ringdown spin expansion coefficients formalism,” *Phys. Rev. D* **103**, 124043 (2021), [arXiv:2102.05939 \[gr-qc\]](#).
- [43] Abhirup Ghosh, Richard Brito, and Alessandra Buonanno, “Constraints on quasinormal-mode frequencies with LIGO-Virgo binary–black-hole observations,” *Phys. Rev. D* **103**, 124041 (2021), [arXiv:2104.01906 \[gr-qc\]](#).
- [44] Carl-Johan Haster, “Pi from the sky – A null test of general relativity from a population of gravitational wave observations,” (2020), [arXiv:2005.05472 \[gr-qc\]](#).
- [45] Yasmeen Asali, Peter T. H. Pang, Anuradha Samajdar, and Chris Van Den Broeck, “Probing resonant excitations in exotic compact objects via gravitational waves,” *Phys. Rev. D* **102**, 024016 (2020), [arXiv:2004.05128 \[gr-qc\]](#).
- [46] Bruce Edelman *et al.*, “Constraining unmodeled physics with compact binary mergers from GWTC-1,” *Phys. Rev. D* **103**, 042004 (2021), [arXiv:2008.06436 \[gr-qc\]](#).
- [47] Dimitrios Psaltis, Colm Talbot, Ethan Payne, and Ilya Mandel, “Probing the Black Hole Metric. I. Black Hole Shadows and Binary Black-Hole Inspirals,” *Phys. Rev. D* **103**, 104036 (2021), [arXiv:2012.02117 \[gr-qc\]](#).
- [48] Swetha Bhagwat and Costantino Pacilio, “Merger-ringdown consistency: A new test of strong gravity using deep learning,” *Phys. Rev. D* **104**, 024030 (2021), [arXiv:2101.07817 \[gr-qc\]](#).
- [49] Abhirup Ghosh, Nathan K. Johnson-Mcdaniel, Archisman Ghosh, Chandra Kant Mishra, Parameswaran Ajith, Walter Del Pozzo, Christopher P. L. Berry, Alex B. Nielsen, and Lionel London, “Testing general relativity using gravitational wave signals from the inspiral, merger and ringdown of binary black holes,” *Class. Quant. Grav.* **35**, 014002 (2018), [arXiv:1704.06784 \[gr-qc\]](#).
- [50] Abhirup Ghosh *et al.*, “Testing general relativity using golden black-hole binaries,” *Phys. Rev. D* **94**, 021101 (2016), [arXiv:1602.02453 \[gr-qc\]](#).
- [51] Maximiliano Isi, Katerina Chatziioannou, and Will M. Farr, “Hierarchical test of general relativity with gravitational waves,” *Phys. Rev. Lett.* **123**, 121101 (2019), [arXiv:1904.08011 \[gr-qc\]](#).
- [52] Maximiliano Isi, Matthew Giesler, Will M. Farr, Mark A. Scheel, and Saul A. Teukolsky, “Testing the no-hair theorem with GW150914,” *Phys. Rev. Lett.* **123**, 111102 (2019), [arXiv:1905.00869 \[gr-qc\]](#).
- [53] Maximiliano Isi, Will M. Farr, Matthew Giesler, Mark A. Scheel, and Saul A. Teukolsky, “Testing the Black-Hole Area Law with GW150914,” *Phys. Rev. Lett.* **127**, 011103 (2021), [arXiv:2012.04486 \[gr-qc\]](#).
- [54] Juan Calderón Bustillo, Paul D. Lasky, and Eric Thrane, “Black-hole spectroscopy, the no-hair theorem, and GW150914: Kerr versus Occam,” *Phys. Rev. D* **103**, 024041 (2021), [arXiv:2010.01857 \[gr-qc\]](#).
- [55] Werner Israel, “Event horizons in static vacuum space-times,” *Phys. Rev.* **164**, 1776–1779 (1967).
- [56] Werner Israel, “Event horizons in static electrovac space-times,” *Commun. Math. Phys.* **8**, 245–260 (1968).
- [57] B. Carter, “Axisymmetric Black Hole Has Only Two Degrees of Freedom,” *Phys. Rev. Lett.* **26**, 331–333 (1971).
- [58] C. V. Vishveshwara, “Scattering of Gravitational Radiation by a Schwarzschild Black-hole,” *Nature* **227**, 936–938 (1970).
- [59] William H. Press, “Long Wave Trains of Gravitational Waves from a Vibrating Black Hole,” *Astrophys. J. Lett.* **170**, L105–L108 (1971).
- [60] S. Chandrasekhar and Steven L. Detweiler, “The quasi-normal modes of the Schwarzschild black hole,” *Proc. Roy. Soc. Lond. A* **344**, 441–452 (1975).
- [61] Olaf Dreyer, Bernard J. Kelly, Badri Krishnan, Lee Samuel Finn, David Garrison, and Ramon Lopez-Aleman, “Black hole spectroscopy: Testing general relativity through gravitational wave observations,” *Class. Quant. Grav.* **21**, 787–804 (2004), [arXiv:gr-qc/0309007](#).
- [62] Emanuele Berti, Vitor Cardoso, and Clifford M. Will, “On gravitational-wave spectroscopy of massive black holes with the space interferometer LISA,” *Phys. Rev. D* **73**, 064030 (2006), [arXiv:gr-qc/0512160](#).
- [63] Emanuele Berti, Jaime Cardoso, Vitor Cardoso, and Marco Cavaglia, “Matched-filtering and parameter estimation of ringdown waveforms,” *Phys. Rev. D* **76**, 104044 (2007), [arXiv:0707.1202 \[gr-qc\]](#).
- [64] S. Gossan, J. Veitch, and B. S. Sathyaprakash, “Bayesian model selection for testing the no-hair theorem with black hole ringdowns,” *Phys. Rev. D* **85**, 124056 (2012), [arXiv:1111.5819 \[gr-qc\]](#).
- [65] Emanuele Berti, Alberto Sesana, Enrico Barausse, Vitor Cardoso, and Krzysztof Belczynski, “Spectroscopy of Kerr black holes with Earth- and space-based interferometers,” *Phys. Rev. Lett.* **117**, 101102 (2016), [arXiv:1605.09286 \[gr-qc\]](#).
- [66] Matthew Giesler, Maximiliano Isi, Mark A. Scheel, and Saul Teukolsky, “Black Hole Ringdown: The Importance of Overtones,” *Phys. Rev. X* **9**, 041060 (2019), [arXiv:1903.08284 \[gr-qc\]](#).

- qc].
- [67] Miriam Cabero, Julian Westerweck, Collin D. Capano, Sumit Kumar, Alex B. Nielsen, and Badri Krishnan, “Black hole spectroscopy in the next decade,” *Phys. Rev. D* **101**, 064044 (2020), arXiv:1911.01361 [gr-qc].
- [68] Maximiliano Isi and Will M. Farr, “Analyzing black-hole ring-downs,” (2021), arXiv:2107.05609 [gr-qc].
- [69] Ryuichi Takahashi and Takashi Nakamura, “Wave effects in gravitational lensing of gravitational waves from chirping binaries,” *Astrophys. J.* **595**, 1039–1051 (2003), arXiv:astro-ph/0305055.
- [70] Enrico Barausse and Luciano Rezzolla, “The Influence of the hydrodynamic drag from an accretion torus on extreme mass-ratio inspirals,” *Phys. Rev. D* **77**, 104027 (2008), arXiv:0711.4558 [gr-qc].
- [71] Nicolas Yunes, Bence Kocsis, Abraham Loeb, and Zoltan Haiman, “Imprint of Accretion Disk-Induced Migration on Gravitational Waves from Extreme Mass Ratio Inspirals,” *Phys. Rev. Lett.* **107**, 171103 (2011), arXiv:1103.4609 [astro-ph.CO].
- [72] Enrico Barausse, Vitor Cardoso, and Paolo Pani, “Can environmental effects spoil precision gravitational-wave astrophysics?” *Phys. Rev. D* **89**, 104059 (2014), arXiv:1404.7149 [gr-qc].
- [73] Enrico Barausse, Vitor Cardoso, and Paolo Pani, “Environmental Effects for Gravitational-wave Astrophysics,” *J. Phys. Conf. Ser.* **610**, 012044 (2015), arXiv:1404.7140 [astro-ph.CO].
- [74] Collin D. Capano and Alexander H. Nitz, “Binary black hole spectroscopy: a no-hair test of GW190814 and GW190412,” *Phys. Rev. D* **102**, 124070 (2020), arXiv:2008.02248 [gr-qc].
- [75] R. Abbott *et al.* (LIGO Scientific, Virgo), “GW190412: Observation of a Binary-Black-Hole Coalescence with Asymmetric Masses,” *Phys. Rev. D* **102**, 043015 (2020), arXiv:2004.08342 [astro-ph.HE].
- [76] Alejandro Bohé *et al.*, “Improved effective-one-body model of spinning, nonprecessing binary black holes for the era of gravitational-wave astrophysics with advanced detectors,” *Phys. Rev. D* **95**, 044028 (2017), arXiv:1611.03703 [gr-qc].
- [77] Roberto Cotesta, Alessandra Buonanno, Alejandro Bohé, Andrea Taracchini, Ian Hinder, and Serguei Ossokine, “Enriching the Symphony of Gravitational Waves from Binary Black Holes by Tuning Higher Harmonics,” *Phys. Rev. D* **98**, 084028 (2018), arXiv:1803.10701 [gr-qc].
- [78] Roberto Cotesta, Sylvain Marsat, and Michael Pürrer, “Frequency domain reduced order model of aligned-spin effective-one-body waveforms with higher-order modes,” *Phys. Rev. D* **101**, 124040 (2020), arXiv:2003.12079 [gr-qc].
- [79] Yi Pan, Alessandra Buonanno, Andrea Taracchini, Lawrence E. Kidder, Abdul H. Mroué, Harald P. Pfeiffer, Mark A. Scheel, and Béla Szilágyi, “Inspiral-merger-ringdown waveforms of spinning, precessing black-hole binaries in the effective-one-body formalism,” *Phys. Rev. D* **89**, 084006 (2014), arXiv:1307.6232 [gr-qc].
- [80] Stanislav Babak, Andrea Taracchini, and Alessandra Buonanno, “Validating the effective-one-body model of spinning, precessing binary black holes against numerical relativity,” *Phys. Rev. D* **95**, 024010 (2017), arXiv:1607.05661 [gr-qc].
- [81] Sascha Husa, Sebastian Khan, Mark Hannam, Michael Pürrer, Frank Ohme, Xisco Jiménez Forteza, and Alejandro Bohé, “Frequency-domain gravitational waves from nonprecessing black-hole binaries. I. New numerical waveforms and anatomy of the signal,” *Phys. Rev. D* **93**, 044006 (2016), arXiv:1508.07250 [gr-qc].
- [82] Sebastian Khan, Sascha Husa, Mark Hannam, Frank Ohme, Michael Pürrer, Xisco Jiménez Forteza, and Alejandro Bohé, “Frequency-domain gravitational waves from nonprecessing black-hole binaries. II. A phenomenological model for the advanced detector era,” *Phys. Rev. D* **93**, 044007 (2016), arXiv:1508.07253 [gr-qc].
- [83] Lionel London, Sebastian Khan, Edward Fauchon-Jones, Cecilia García, Mark Hannam, Sascha Husa, Xisco Jiménez-Forteza, Chinmay Kalaghatgi, Frank Ohme, and Francesco Pannarale, “First higher-multipole model of gravitational waves from spinning and coalescing black-hole binaries,” *Phys. Rev. Lett.* **120**, 161102 (2018), arXiv:1708.00404 [gr-qc].
- [84] Sebastian Khan, Katerina Chatziioannou, Mark Hannam, and Frank Ohme, “Phenomenological model for the gravitational-wave signal from precessing binary black holes with two-spin effects,” *Phys. Rev. D* **100**, 024059 (2019), arXiv:1809.10113 [gr-qc].
- [85] Mark Hannam, Patricia Schmidt, Alejandro Bohé, Leila Haegel, Sascha Husa, Frank Ohme, Geraint Pratten, and Michael Pürrer, “Simple Model of Complete Precessing Black-Hole-Binary Gravitational Waveforms,” *Phys. Rev. Lett.* **113**, 151101 (2014), arXiv:1308.3271 [gr-qc].
- [86] Sebastian Khan, Frank Ohme, Katerina Chatziioannou, and Mark Hannam, “Including higher order multipoles in gravitational-wave models for precessing binary black holes,” *Phys. Rev. D* **101**, 024056 (2020), arXiv:1911.06050 [gr-qc].
- [87] Vijay Varma, Scott E. Field, Mark A. Scheel, Jonathan Blackman, Davide Gerosa, Leo C. Stein, Lawrence E. Kidder, and Harald P. Pfeiffer, “Surrogate models for precessing binary black hole simulations with unequal masses,” *Phys. Rev. Research* **1**, 033015 (2019), arXiv:1905.09300 [gr-qc].
- [88] Vijay Varma, Scott E. Field, Mark A. Scheel, Jonathan Blackman, Lawrence E. Kidder, and Harald P. Pfeiffer, “Surrogate model of hybridized numerical relativity binary black hole waveforms,” *Phys. Rev. D* **99**, 064045 (2019), arXiv:1812.07865 [gr-qc].
- [89] Tousif Islam, Vijay Varma, Jackie Lodman, Scott E. Field, Gaurav Khanna, Mark A. Scheel, Harald P. Pfeiffer, Davide Gerosa, and Lawrence E. Kidder, “Eccentric binary black hole surrogate models for the gravitational waveform and remnant properties: comparable mass, nonspinning case,” *Phys. Rev. D* **103**, 064022 (2021), arXiv:2101.11798 [gr-qc].
- [90] Vijay Varma and Parameswaran Ajith, “Effects of non-quadrupole modes in the detection and parameter estimation of black hole binaries with nonprecessing spins,” *Phys. Rev. D* **96**, 124024 (2017), arXiv:1612.05608 [gr-qc].
- [91] Juan Calderón Bustillo, Sascha Husa, Alicia M. Sintes, and Michael Pürrer, “Impact of gravitational radiation higher order modes on single aligned-spin gravitational wave searches for binary black holes,” *Phys. Rev. D* **93**, 084019 (2016), arXiv:1511.02060 [gr-qc].
- [92] Collin Capano, Yi Pan, and Alessandra Buonanno, “Impact of higher harmonics in searching for gravitational waves from non-spinning binary black holes,” *Phys. Rev. D* **89**, 102003 (2014), arXiv:1311.1286 [gr-qc].
- [93] Tyson B. Littenberg, John G. Baker, Alessandra Buonanno, and Bernard J. Kelly, “Systematic biases in parameter estimation of binary black-hole mergers,” *Phys. Rev. D* **87**, 104003 (2013), arXiv:1210.0893 [gr-qc].
- [94] Juan Calderón Bustillo, Pablo Laguna, and Deirdre Shoemaker, “Detectability of gravitational waves from binary black holes: Impact of precession and higher modes,” *Phys. Rev. D* **95**, 104038 (2017), arXiv:1612.02340 [gr-qc].
- [95] Duncan A. Brown, Prayush Kumar, and Alexander H. Nitz, “Template banks to search for low-mass binary black holes in advanced gravitational-wave detectors,” *Phys. Rev. D* **87**, 082004 (2013), arXiv:1211.6184 [gr-qc].



- [96] V. Varma, P. Ajith, S. Husa, J. C. Bustillo, M. Hannam, and M. Pürrer, “Gravitational-wave observations of binary black holes: Effect of nonquadrupole modes,” *Phys. Rev. D* **90**, 124004 (2014), arXiv:1409.2349 [gr-qc].
- [97] Philip B. Graff, Alessandra Buonanno, and B. S. Sathyaprakash, “Missing Link: Bayesian detection and measurement of intermediate-mass black-hole binaries,” *Phys. Rev. D* **92**, 022002 (2015), arXiv:1504.04766 [gr-qc].
- [98] Ian Harry, Juan Calderón Bustillo, and Alex Nitz, “Searching for the full symphony of black hole binary mergers,” *Phys. Rev. D* **97**, 023004 (2018), arXiv:1709.09181 [gr-qc].
- [99] Katerina Chatziioannou *et al.*, “On the properties of the massive binary black hole merger GW170729,” *Phys. Rev. D* **100**, 104015 (2019), arXiv:1903.06742 [gr-qc].
- [100] Feroz H. Shaik, Jacob Lange, Scott E. Field, Richard O’Shaughnessy, Vijay Varma, Lawrence E. Kidder, Harald P. Pfeiffer, and Daniel Wysocki, “Impact of subdominant modes on the interpretation of gravitational-wave signals from heavy binary black hole systems,” *Phys. Rev. D* **101**, 124054 (2020), arXiv:1911.02693 [gr-qc].
- [101] Tousif Islam, Scott E. Field, Carl-Johan Haster, and Rory Smith, “High-precision source characterization of intermediate mass-ratio black hole coalescences with gravitational waves: The importance of higher-order multipoles,” (2021), arXiv:2105.04422 [gr-qc].
- [102] Nathan K. Johnson-McDaniel, Abhirup Ghosh, Sudarshan Ghonge, Muhammed Saleem, N. V. Krishnendu, and James A. Clark, “Investigating the relation between gravitational wave tests of general relativity,” (2021), arXiv:2109.06988 [gr-qc].
- [103] E. T. Newman and R. Penrose, “Note on the Bondi-Metzner-Sachs group,” *J. Math. Phys.* **7**, 863–870 (1966).
- [104] I. M. Romero-Shaw *et al.*, “Bayesian inference for compact binary coalescences with bilby: validation and application to the first LIGO–Virgo gravitational-wave transient catalogue,” *Mon. Not. Roy. Astron. Soc.* **499**, 3295–3319 (2020), arXiv:2006.00714 [astro-ph.IM].
- [105] J. Veitch and A. Vecchio, “Bayesian coherent analysis of inspiral gravitational wave signals with a detector network,” *Phys. Rev. D* **81**, 062003 (2010), arXiv:0911.3820 [astro-ph.CO].
- [106] Gregory Ashton *et al.*, “BILBY: A user-friendly Bayesian inference library for gravitational-wave astronomy,” *Astrophys. J. Suppl.* **241**, 27 (2019), arXiv:1811.02042 [astro-ph.IM].
- [107] Rory Smith, Gregory Ashton, Avi Vajpeyi, and Colm Talbot, “Massively parallel Bayesian inference for transient gravitational-wave astronomy,” ArXiv e-prints (2019), arXiv:1909.11873 [gr-qc].
- [108] Joshua S. Speagle, “DYNesty: a dynamic nested sampling package for estimating Bayesian posteriors and evidences,” *Mon. Not. Roy. Astron. Soc.* **493**, 3132–3158 (2020), arXiv:1904.02180 [astro-ph.IM].
- [109] LIGO Scientific Collaboration and Virgo Collaboration, “The GW190814 Data Release,” (2020).
- [110] Tyson B. Littenberg and Neil J. Cornish, “Bayesian inference for spectral estimation of gravitational wave detector noise,” *Phys. Rev. D* **91**, 084034 (2015), arXiv:1410.3852 [gr-qc].
- [111] Neil J. Cornish and Tyson B. Littenberg, “BayesWave: Bayesian Inference for Gravitational Wave Bursts and Instrument Glitches,” *Class. Quant. Grav.* **32**, 135012 (2015), arXiv:1410.3835 [gr-qc].
- [112] Katerina Chatziioannou, Carl-Johan Haster, Tyson B. Littenberg, Will M. Farr, Sudarshan Ghonge, Margaret Millhouse, James A. Clark, and Neil Cornish, “Noise spectral estimation methods and their impact on gravitational wave measurement of compact binary mergers,” *Phys. Rev. D* **100**, 104004 (2019), arXiv:1907.06540 [gr-qc].
- [113] Geraint Pratten *et al.*, “Let’s twist again: computationally efficient models for the dominant and sub-dominant harmonic modes of precessing binary black holes,” (2020), arXiv:2004.06503 [gr-qc].
- [114] Geraint Pratten, Sascha Husa, Cecilio Garcia-Quiros, Marta Colleoni, Antoni Ramos-Buades, Hector Estelles, and Rafel Jaume, “Setting the cornerstone for a family of models for gravitational waves from compact binaries: The dominant harmonic for non precessing quasi-circular black holes,” *Phys. Rev. D* **102**, 064001 (2020), arXiv:2001.11412 [gr-qc].
- [115] Cecilio García-Quiros, Marta Colleoni, Sascha Husa, Héctor Estellés, Geraint Pratten, Antoni Ramos-Buades, Maite Mateu-Lucena, and Rafel Jaume, “Multimode frequency-domain model for the gravitational wave signal from nonprecessing black-hole binaries,” *Phys. Rev. D* **102**, 064002 (2020), arXiv:2001.10914 [gr-qc].
- [116] Roberto Cotesta, Sylvain Marsat, and Michael Pürrer, “Frequency domain reduced order model of aligned-spin effective-one-body waveforms with higher-order modes,” *Phys. Rev. D* **101**, 124040 (2020), arXiv:2003.12079 [gr-qc].
- [117] Lionel London, Sebastian Khan, Edward Fauchon-Jones, Cecilio García, Mark Hannam, Sascha Husa, Xisco Jiménez-Forteza, Chinmay Kalaghatgi, Frank Ohme, and Francesco Pannarale, “First higher-multipole model of gravitational waves from spinning and coalescing black-hole binaries,” *Phys. Rev. Lett.* **120**, 161102 (2018), arXiv:1708.00404 [gr-qc].
- [118] LIGO Scientific Collaboration, “LIGO Algorithm Library - LALSuite,” free software (GPL) (2020).
- [119] Peter T. H. Pang, Juan Calderón Bustillo, Yifan Wang, and Tjonnie G. F. Li, “Potential observations of false deviations from general relativity in gravitational wave signals from binary black holes,” *Phys. Rev. D* **98**, 024019 (2018), arXiv:1802.03306 [gr-qc].
- [120] Rich Abbott *et al.* (LIGO Scientific, Virgo), “Open data from the first and second observing runs of Advanced LIGO and Advanced Virgo,” *SoftwareX* **13**, 100658 (2021), arXiv:1912.11716 [gr-qc].